HHS Public Access

Author manuscript

J Immunol. Author manuscript; available in PMC 2017 March 15.

Published in final edited form as:

J Immunol. 2016 March 15; 196(6): 2870–2878. doi:10.4049/jimmunol.1502027.

Enhanced cytotoxic CD8 T cell priming using DC expressing HPV-16 E6/E7-p16^{INK4} fusion protein with sequenced anti-PD1

Tatiana M. Garcia-Bates[*,§], **Eun Kim**[†], **Fernando Concha-Benavente**[‡], **Sumita Trivedi**[*], **Robbie B. Mailliard**[§], **Andrea Gambotto**[†], and **Robert L. Ferris**[*,‡,¶]

[*]Department of Otolaryngology, University of Pittsburgh, Pittsburgh, PA, USA

[†]Department of Surgery, University of Pittsburgh, Pittsburgh, PA, USA

[‡]Department of Immunology, University of Pittsburgh, Pittsburgh, PA, USA

[§]Department of Infectious Diseases and Microbiology, Graduate School of Public Health, University of Pittsburgh, Pittsburgh, PA, USA

[¶]Cancer Immunology Program, University of Pittsburgh Cancer Institute, Pittsburgh, PA, USA

Abstract

The incidence of human papillomavirus (HPV)-related head and neck squamous cell carcinoma (HNSCC) has increased in recent decades, though HPV prevention vaccines may reduce this rise in the future. HPV related cancers express the viral oncoproteins E6 and E7. The latter inactivates the tumor suppressor protein retinoblastoma (Rb), which leads to the overexpression of p16^{INK4} protein, providing unique antigens for therapeutic HPV-specific cancer vaccination. We developed potential adenoviral vaccines that express a fusion protein of HPV-16 E6 and E7 (Ad.E6E7) alone or fused with p16 (Ad.E6E7p16), and also encoding an anti-programmed death (PD)-1 antibody. Human monocyte-derived dendritic cells (DC) transduced with Ad.E6E7 or Ad.E6E7p16 with or without Ad.αPD1 were used to activate autologous CD8 cytotoxic T lymphocytes (CTL) *in vitro*. CTL responses were tested against naturally HPV-infected HNSCC cells using IFNγ ELISPOT and ^{51}Cr release assay. Surprisingly, stimulation and antitumor activity of CTL were increased after incubation with Ad.E6E7p16-transduced DC (DC.E6E7p16) compared to Ad.E6E7 (DC.E6E7), a result that may be due to an effect of p16 on CDK4 levels and IL-12 secretion by DC. Moreover, the beneficial effect was most prominent when anti-PD1 was introduced during the second round of stimulation (after initial priming). These data suggest that careful sequencing of Ad.E6E7.p16 with Ad.αPD1 could improve anti-tumor immunity against HPV-related tumors and that p16 may enhance the immunogenicity of DC, through cyclin-dependent pathways, Th1 cytokine secretion and by adding a non-viral antigen highly overexpressed in HPV-induced cancers.

Corresponding author: Robert L. Ferris, MD, PhD; Hillman Cancer Center Research Pavilion, 5117 Centre Avenue, Room 2.26b, Pittsburgh, PA USA 15213-1863. Phone: 412-623-0327, Fax: 412-623-4840, ferrisrl@upmc.edu.

There are no conflicts of interest.

Introduction

The incidence of human papillomavirus positive (HPV+) head and neck squamous cell carcinoma (HNSCC), especially oropharyngeal carcinoma (OPC) have been rising over recent decades and now accounts for 70–80% of OPC in the United States and Europe (1–4). Even though the overall survival of HPV+ cancers is better than the HPV negative counterparts, the increasing incidence demands the discovery of more targeted therapies harnessing unique tumor-associated antigens (TAA).

HPV+ cancers have unique expression of virally encoded proteins that can be used as therapeutic targets. The main oncogenic proteins E6 and E7 are continuously expressed and are necessary for the maintenance of malignant transformation (5). Our laboratory previously evaluated the endogenous level of circulating HPV type 16 E7-specific T cells in HPV+ cancer patients, showing a marked increase in HPV E7-specific T cells in the circulation compared to HPV negative patients. These T cells were able to recognize the naturally HPV-infected SCC-90 HNSCC cells (6). Despite this finding of anti-HPV immunity, T cells are driven into a terminally differentiated phenotype and tumor progression still occurs. Therefore, therapeutic vaccine strategies to induce immunogenicity and reverse exhaustion within the tumor microenvironment are critical for improved survival.

In HPV+ head and neck cancers, E6 and E7 oncoproteins have been used as therapeutic targets with encouraging results when combined with the current treatments of cisplatin and radiation (7–10). In normal tissues, $p16^{INK4}$ (p16) is known as a tumor suppressor that regulates cell-cycle progression by inhibiting the cyclin-dependent kinases CDK4 and CDK6 and consequently inhibiting Rb phosphorylation and further proteasomal degradation (11). However, in HPV+ HNSCC, p16 protein is strongly overexpressed due to the loss of Rb caused by the E7 oncoprotein (12). This key feature also makes p16 a potential TAA for vaccine therapies.

In addition to using viral and TAA to induce cellular T cell responses, it is also imperative to target the inhibitory signals that may hinder their activity, such as the co-inhibitory receptor on T cells, PD-1. Therefore in this study, we developed adenoviral vectors expressing non-oncogenic (mutated) E6 and E7 genes as a single hybrid gene or fused with $p16^{INK4}$ gene as a therapeutic viral vaccine. Moreover, we compared these vectors alone or in combination with an adenovirus expressing the anti-PD1 monoclonal antibody (mAb) to further enhance cellular anti-HPV immune responses against HNSCC and we tested the optimal sequence of anti-PD1 combination with T cell expansion. We investigated surprising observation that p16 may have a salutary effect on DC stimulation through Th1 cytokine secretion and its effect on CDK4 levels, in addition to enhancing overall CD8 T cell responses against HPV-infected tumor cells.

Materials and Methods

Cell lines

HPV+ HNSCC SCC-90 and HPV-negative HNSCC PCI-13 were derived from patients treated at University of Pittsburgh Cancer Institute and characterized previously (6, 13). Cells were grown in Iscove's modified Dulbecco's medium (IMDM, Sigma) in the presence of 10% fetal bovine serum (FBS, Cellgro), 2% L-glutamine and 1% penicillin/streptomycin (Invitrogen) and incubated at 37°C in 5% CO_2

Design of codon optimized adenoviruses expressing HPV 16 E6 and E7 alone or fused with $p16^{INK4}$

The HPV oncoproteins E6 and E7 are known to initiate malignant transformation by inactivating the tumor suppressors p53 and retinoblastoma (Rb) respectively (5, 14). In order to use these oncoproteins as immune therapeutic targets without causing transformation of the dendritic cell (DC), we introduced genetic alterations in the E6 and E7 genes. The two mutations in E6 (L50G and G130V) disable its ability to degrade p53 (15, 16). The mutation on E7 (H2P) and the deletion of amino acids 21 to 24 (Δ21–24) prevent its binding and inactivation of pRb (17). The gene of HPV 16 E6E7 fusion protein (E6; GenBank AF486315.1, E7; GenBank AF486326.1) mutated L57G and G137V on E6 and H2P and Δ21–24 on E7 was codon-optimized for optimal expression in mammalian cells using the UpGene codon optimization algorithm (18). Three genes with no significant similarity between any two genes having Sal I site in 5′ end and BamH I-TGA-Not I in 3′ end were synthesized (GenScript). Ad.E6E7-1, Ad.E6E7-2, and Ad.E6E7-3 were generated by subcloning the codon-optimized genes into the shuttle vector, pAdlox (GenBank U62024), at Sal I/Not I sites. The coding sequence of p16 (GenBank NP000068.1) having Sal I and Bgl II sites in 5′ end and BamH I-TGA-Not I in 3′ end was also codon-optimized, synthesized, and generated as Ad.p16. To fuse E6E7 gene with p16 gene, p16 gene digested Bgl II and Not I was cloned into Ad.E6E7-2 digested with BamH I and Not I and generated as Ad.E6E7p16 (Supplementary Fig. 1A). Replication-defective human adenovirus serotype 5, designated as Ad.E6E7-1, Ad.E6E7-2 Ad.E6E7-3, and Ad.E6E7p16 were generated by loxP homologous recombination on HEK-293 cells and purified by CsCl banding, followed by dialysis in 3% sucrose solution. As controls, the empty adenoviral vector was used (Ad.Ψ5) or the Ad.p16 was used. Infectious titers were determined using quantitative real-time PCR as previously described and were approximately 100-fold less than particle titers (19). Viruses were aliquoted and stored at −80°C until use.

Characterization of Ad.E6E7 and Ad.E6E7p16 expression on human cells

To evaluate the expression of these fused proteins *in vitro*, control HPV negative SCCHN PCI-13 cells were left untreated (mock) or were infected at different multiplicity of infections (MOI) (10 and 50) with the three E6E7 containing vectors (Ad.E6E7-1, Ad.E6E7-2 and Ad.E6E7-3), Ad.E6E7p16 or Ad.p16 for 48 hours. In order to select the optimal (highest) antigen-expressing vector, cell lysates were collected and western blot analysis was performed to detect E7 (Supplementary Fig. 1B, left panel) and p16 protein (Supplementary Fig. 1B, right panel). PCI-13 cells transduced with the three Ad.E6E7 vectors and the Ad.E6E7p16 contained abundant E7 protein at the appropriate molecular

weight (31 KDa for E6E7 alone or 44 KDa for the fused E6E7p16). The levels of p16 were also detected in the cells that were transduced with Ad.p16 alone or Ad.E6E7p16 (Supplementary Fig.1B). All vectors showed high levels of expression in these cells especially at an MOI of 50. Transgene expression was also tested in mDC. Previous reports that use adenoviral-vectors to deliver transgenes to dendritic cells have use MOIs that vary from 100 to 1000 (20, 21). We therefore tested three different MOIs (250, 500 and 1000) to assess transgene expression and toxicity. We observed that all three Ad.E6E7 constructs yielded high levels of transduction efficacy and viability was not compromised at the lower MOIs of 250 and 500 (Supplementary Fig. 1C, 1D and 1E), with the 1000 MOI having the highest amount of protein of all three with slight increase in cell toxicity (Supplementary Fig. 1C, 1D and 1E). However, the Ad.E6E7 construct # 2 (Ad.E6E7-2) had the highest expression. Therefore for future experiments we selected that construct. We were also able to detect high levels of expression of the fusion protein of E6E7 and p16, which yielded a protein at a molecular weight of 44 KDa (Supplementary Fig. 1C, right panel). For all the experiments that follow, an MOI of 500 was chosen for its high level of antigen expression and lower toxicity to infected cells.

Stable cell line expressing hPD1

The coding sequence for human PD1 (GenBank NP005009.2) and near-infrared fluorescent protein (iRFP, GenBank AEL88490.1) (19) was codon-optimized for optimal expression in mammalian cells using the UpGene codon optimization algorithm (18) and synthesized (GenScript). Eag I and BstB I sites for hPD1 and Sal I and BamH I sites for iRFP were generated at the 5′ and 3′ ends to clone each gene into the Not I and BstB I site under the EF-1 promoter and Sal I and BamH I sites under the cytomegalovirus (CMV) promoter of pBUDCE4.1 mammalian expression vector (Invitrogen), respectively. A Kozak sequence was also generated at the 5′ end. The resulting plasmid containing both hPD1 and iRFP gene was named pBudCE4.1/iRFP-hPD1.

Plasmid pBudCE4.1/iRFP-hPD1 was used to transfect HEK-293 cells using the Lipofectamine 2000 transfection reagent (Invitrogen) according to the manufacturer's recommendations. After 24 h, cells were passaged at 1:20 dilution into fresh growth medium (Dulbecco's modified Eagle's medium containing 10% fetal bovine serum) with Zeocin antibiotic (InvivoGen) for selective pressure. Medium containing 100 μg/ml Zeocin was changed after every 3–4 days for 4 weeks. Resistant colonies were pooled and clonal lines were obtained by cell sorting those that produced iRFP using Cy5.5 filter set (665/45 nm exciter and 725/50 nm emitter) in FACSAria (BD Sciences). After the selection, the stable cell line was termed 293/PD1 and had expression of both hPD1 and iRFP. Cells were maintained at 50 μg/ml of Zeocin in Dulbecco's modified Eagle's medium containing 10% fetal bovine serum. Frozen stocks were made.

Design and characterization of Ad.αPD1 and its secretion by human DC

To enhance the generation of tumor antigen-specific cytotoxic CD8 T cells, we also constructed an adenovirus expressing an anti-PD1 mAb, to target this co-inhibitory checkpoint receptor on T cells. For the recombinant adenovirus expressing human anti-PD1 antibody, heavy chain gene (HC) was codon-optimized, synthesized, and cloned into Sal I

and Not I site of pAdlox and generated as pAd.HC. The light chain gene (LC) having Eag I and Kpn I site in 5′ end and Swa I and BstB I was codon-optimized, synthesized, and cloned into Not I and Bst B I site of pBudCE4.1 (Invitrogen) and generated as pBud.LC. The gene cassette of EF-1 promoter-LC-BGH polyadenylation sequence was prepared by digested with Nhe I and Drd I following the klenow treatment and cloned into Pvu II site of pAd/HC generated as Ad.αhPD1 (Supplementary Fig. 2A). To exchange the signal peptide of human IgG4 with that of mouse IgG, HC and LC were amplified with mspHC-S (5'GATGTCGACGCCACCATGGCTGTCCTTGGCCTCCTGTTCTGCCTCGT GACGTTTCCCTCATGCGTGCTGTCGCAGGTGCAGCTCGTGGAGAGCGGG-3') and Ad-R (5'-GTAACCATTATAAGCTGC-3') primers and mspLC-S (5'-GCCGGTACCGCCAC CATGGTGTCTACCCCTCAGTTCCTGGTGTTCCTGCTCTTCTGGATTCCGGCTTCCA GGGGCGACATCCTGCTGACTCAGTCTCCGGCCACCCTC-3') and BGH-R (5'-TAGAAGGCACAGTCGAGG-3') primers, respectively. The mspHC PCR product digested with Sal I and Not I and the mspLC PCR product digested with Kpn I and Swa I replaced the HC or LC gene in Ad.αhPD1 serially, and the vector termed Ad.msp-αhPD1 (Supplementary Fig. 2A). All constructions were confirmed by sequencing. Subsequently, replication-defective human adenovirus serotype 5, designated as Ad.αhPD1 and Ad.msp-αhPD1, were generated by loxP homologous recombination on HEK-293 cells and purified and stored as described previously.

Evaluation of binding of anti-hPD1 to surface PD1 on 293/PD1

Before making the adenoviral construct, the plasmids were evaluated for the proper folding of the antibody and secretion from the cell. First, 293 cells were transfected with either a control empty vector or the two constructs (αhPD1 and msp-αhPD1) for 72 hours. We then added the relevant supernatants to 293 cells that express PD1 on the surface (293/PD1). After a 1 hour incubation, the binding of the anti-PD1 antibody was tested by the addition of two secondary antibodies, one against human IgG4 (Biotin-αIgG4-avidin PE) and one against whole human IgG conjugated to FITC (αhIgG FITC). We were able to detect between 70%–72% IgG positive cells when the αhPD1 without the mouse signal peptide was used. When we used a vector encoding a mouse signal peptide (msp.αPD1), a greater percentage of IgG4 (79%) and IgG (80%) positive cells was detected than when αhPD1 without mouse signal peptide was used (Supplementary Fig. 2B). After the respective adenoviruses were packaged and titered, we then tested the adenovirus in both immature DC (iDC) and mature DC (mDC). Immature DC (iDC) and mature DC (mDC) were transduced at an MOI of 500 for 72 hours and supernatants were collected. These supernatants were then added to 293/PD1 cells and we observed that both the Ad.αhPD1 and the Ad.msp.αPD1 were secreted from adenovirus-transduced iDCs (85 % from DC.αPD1 and 86% from DC.mspαPD1, respectively). However, when the same vectors were use in mDCs, the Ad.msp.αPD1-transduced mDC (DC.msp.αPD1) showed a greater proportion of IgG positive cells (83%) than the Ad.αhPD1-transduced mDC alone (DC.αPD1, 53%) (Supplementary Fig. 2C). Therefore, we chose the Ad.msp.αPD1 for the *in vitro* stimulation of CD8 T cells and for brevity we will use the connotation DC.αPD1 for the rest of the manuscript. Mature DC were also evaluated for the expression of maturation markers (CD80 and CD83) after 72 hours post-infection. We did not observed any significant changes on the

presence of CD80 or CD83 in the presence of anti-PD1 (DC.αPD1) compared to mock-infected DC (DC.Mock) or Ad.Ψ5-infected DC (DC.Ψ5) (Supplementary Fig. 3A). We also tested these adenovirus-transduced DC for their ability to produce IL-12, IL-10 and TNFα in the presence of CD40L-transfected J558 cells (provided by Dr. P. Lane, Birmingham, UK) (22). We did not observe a significant change in the amount of these cytokines in the presence of anti-PD1 (Supplementary Fig. 3B). These results suggest that anti-PD1 does not have an effect on the ability of DC to produce these cytokines upon stimulation. Human IL-10 and TNFα ELISA Kits were purchased from Thermo-Scientific.

Generation of human monocyte-derived dendritic cells

Peripheral blood mononuclear cells (PBMC) were isolated from HLA-A2$^+$ healthy donors using Ficoll-Paque PLUS gradient centrifugation (GE Healthcare Life Sciences, Piscataway, NJ). Monocytes were then isolated using EasySep™ Human CD14 Positive selection kit (Stemcell technologies, Vancouver, BC, Canada) and cultured for 5 days in the presence of 1000 IU/ml of GMCSF (R&D systems, Minneapolis, MN) and 1000 IU/ml of IL-4 (R&D systems, Minneapolis, MN) to differentiate them into immature dendritic cells (iDC). These iDC were then collected and the purity was assessed by flow cytometry giving more than 90% purity according to the expression of CD11c, HLAD-DR and the loss of CD14 expression (data not shown). On day 5, an αDC1-polarizing cocktail was added containing IL-1α (25ng/ml), TNFα (50ng/ml), IFNα (3,000 IU/ml) (R&D systems), IFNγ (1,000 IU/ml) (Miltenyi Biotech) and Poly I:C (20μg/ml) (Sigma/Aldrich) for an additional 36 hours to generate mature DC (mDC) as previously described (23). mDCs were then transduced with different adenovirus vector at indicated MOIs for 2 hours at 37C before using them for *in vitro* stimulation of CD8 T cells.

In vitro stimulation of HPV-specific CD8$^+$ T cells using autologous adenovirus-infected DC

CD8$^+$ T cells were negatively selected from PBMC using an EasySep™ human CD8$^+$ T cell enrichment kit (Stemcell technologies, Vancouver, BC, Canada). Briefly, 5×10^4 adenovirus-transduced mDC were use as stimulators of 5×10^5 autologous CD8$^+$ T cells (1:10 DC to T cell ratio) in the presence of CD40L-transfected J558 cells (provided by Dr. P. Lane, Birmingham, UK)(22). After 3 days of stimulation, 50 IU/ml of IL-2 and 10 ng/ml of IL-7 (R&D systems) were added to the cultures. On day 12 of stimulation, T cells were counted and added to newly adenovirus-infected DCs at a 1:10 ratio for an additional 12 days. IL-2 and IL-7 were kept in the cultures and replaced every 3–4 days. When isolating naïve versus memory CD8+ T cells an EasySep™ Human Naïve CD8+ T cell enrichment kit or a EasySep™ Human Memory CD8+ T cell enrichment kit were used.

^{51}Cr release assay

Cytotoxicity using CD8$^+$ T cells was determined using a ^{51}Cr release assay. Briefly, target HNSCC SCC-90 cells were incubated in 100 μL of media with 25 μCi of Na2 51CrO4 (Perkin Elmer, Boston MA) for 60 min at 37°C and resuspended in RPMI 1640 medium supplemented with 25 mM HEPES. Labeled SCC-90 cells were thoroughly washed and plated alone or in the presence of effector CD8$^+$ T cells expanded under the different conditions at a 1:20 Target:Effector (T:E) ratio in 96-well plates. Plates were incubated for 4

h at 37°C in a 5% CO_2 atmosphere. Controls for spontaneous (cells only) and maximal lysis (cells treated with 1% Triton-X) were also included. Each reaction was done in triplicate and the supernatants were collected and analyzed with a Perkin Elmer 96-well plate gamma counter. Results were normalized with the formula lysis = (experimental lysis − spontaneous lysis)/(experimental lysis − maximal lysis) × 100 and results are shown as fold change of specific lysis over Ad.Ψ5.

Western blots

Whole-cell extracts were collected using RIPA buffer (Abcam) with the addition of cOmplete mini protease inhibitors (Sigma-Aldrich) and total protein was quantified using Bradford Assay Kit (Pierce). Twenty to thirty micrograms of protein was electrophoresed through a 4% to 12% SDSPAGE gel (Lonza) and transferred to a polyvinylidene difluoride membrane (Millipore). The membranes were then analyzed for immunoreactivity with the indicated antibodies.

Antibodies and reagents

Mouse monoclonal anti-HPV E7 (clone NM2) and anti-p16 (clone 50.1) were purchased from Santa Cruz Biotechnology. Rabbit mAb anti-CDK4 (D9G3E) and Rabbit anti-Cyclin D1 were purchased from Cell signaling technology. The CDK4/6 inhibitor IV (CAS 359886-84-3) was from Santa Cruz biotechnology.

Antibody staining and flow cytometry

Cells were staining with Ab against cell surface Ag CD3 (clone UCHT1, BD Bioscience), CD8 (clone RPA-T8, Biolegend), PD-1 (clone J105, eBioscience) and CD69 (Clone CH/4, Life technologies). For pentamer staining, a Pro5® MHC class I pentamer was used (A*02:01 YMLDLQPETT, HPV 16 E7 11–20, Proimmune). An amine-reactive viability dye was used to distinguish between live and dead cells (Zombie Aqua Fixable Viability Dye, Biolegend). All samples were acquired on an LSRFortessa (BD Biosciences) flow cytometer, and data were analyzed using FlowJo software (Tree Star).

IL-12 ELISA

Mature monocyte-derived dendritic cells were generated as described earlier in this manuscript. mDC were either mock infected or infected with Ad.Ψ5, Ad.E6E7, Ad.E6E7p16 or Ad.p16 at an MOI of 500. An additional condition was included with simultaneous infection with Ad.E6E7 and 1μM of CDK4 inhibitor. After 24 hr treatment/infection, mDC were harvested and counted. Twenty thousand infected mDC were then added to 96 well plates and 50,000 CD40L-expressing J558 cells were added to stimulate IL-12 secretion. After 48 hrs, supernatants were collected and IL-12 was measured using an IL-12 ELISA kit (Pierce) following the manufacture's protocol.

IFNγ Enzyme-linked immunospot assay (ELISPOT)

The IFNγ ELISPOT was performed following the Mabtech Human IFNγ ELISpot^{Basic} protocol (Mabtech, Cincinnati, OH) using a 96-well PVDF ELISPOT plates from Millipore. Plates were coated with 10 μg/ml of anti-human IFNγ monoclonal antibody 1-D1K

overnight at 4°C. The next day, the coating antibody was washed and plates were blocked with IMDM containing 10% inactivated human AB serum for 2 hours. SCCHN SCC-90 cells were used as targets and were added to the plates at a cell concentration of 2000 cells per well. 20,000 *in vitro*-expanded $CD8^+$ T cells were then added to the wells giving a final Target to T cell ratio of 1:10. Plates were then incubated for 18–20 hours at 37°C, after which they were washed with 1X PBS containing 0.05% Tween-20 (PBS-0.05%Tween-20). Plates were then incubated with the detection anti-human IFNγ biotinylated antibody 7-B6-1 biotin diluted in 1X PBS with 0.5% BSA (1μg/ml, MabTech) for 2 hours at 37°C. After incubation, plates were washed with PBS-0.05%Tween-20 and then a 1:1000 dilution of a streptavidin-conjugated Horseradish Peroxidase (HRP) (MabTech) was added and incubated for 1 hr at 37°C. Finally, 100 μl of TMB substrate was used to develop the spots and numeration of spots was performed using a CTL ImmunoSpot reader and counting software (Cellular Technologies). IFNγ background secretion by T cells alone was subtracted from the final results and was shown as fold change over Ad.Ψ5 control.

Statistical analysis

Statistical analysis was performed using GraphPad Prism 6.0. A two-tailed unpaired or paired *t* test was used and statistical significance was defined as <0.05.

Results

Adenovirus-encoded anti-PD1 effectively blocks PD1 on $CD8^+$ T cells to the same extent as soluble anti-PD1 antibody

To confirm that the Ad-encoded anti-PD1 (mAb) secreted by the DC binds to the PD-1 receptor on activated $CD8^+$ T cells, we performed flow cytometric analysis on the CD8 T cells during a single 12 days *in vitro* stimulation. Briefly, mDC derived from an HLA-A2+ donor were infected with Ad.Ψ5 (DC.Ψ5), Ad.E6E7 (DC.E6E7) or Ad.E6E7p16 (DC.E6E7p16) alone or co-infected with Ad.E6E7 and Ad.αPD1 (DC.E6E7.αPD1) or Ad.E6E7p16 and Ad.αPD1 (DC.E6E7p16.αPD1) at an MOI of 500. These adenovirus-transduced mDCs were then added to autologous purified $CD8^+$ T cells at a ratio of 1:10 (DC:T). To compare the blocking capacity of Ad-encoded anti-PD1 with that of soluble anti-PD1 Ab (nivolumab, Bristol-Myers Squib), we added either hIgG4 as a control (DC.E6E7.hIgG4 and DC.E6E7p16.hIgG4) or anti-PD1 nivolumab (DC.E6E7.Nivo and DC.E6E7p16.Nivo) to the *in vitro* cultures. When $CD8^+$ T cells were stimulated with either DC.Ψ5, DC.E6E7 or DC.E6E7p16 alone or in the presence of hIgG4 control Ab, the levels of PD1 increased overtime, with a peak expression at day 7 of *in vitro* stimulation. However, when $CD8^+$ T cells were stimulated using Ad-αPD1-transduced DC (DC.E6E7.αPD1 or DC.E6E7p16.αPD1), the surface staining with anti-PD1 was blocked almost completely showing in most cases about 5% or less $PD1^+$ $CD8^+$ T cells (Figure 1). Moreover, when we compared the anti-PD1 secreted by Ad-αPD1-transduced DCs with the soluble anti-PD-1 Ab (DC.E6E7.Nivo or DC.E6E7p16.Nivo), we observed that they function with similar potency at blocking PD1 on CD8+ T cells (Figure 1).

Evaluation of CD8+ T cell specificity after *in vitro* stimulation with autologous Ad-transduced mDCs

We next evaluated the specificity of the *in vitro* generated CD8+ T cells against an immunodominant HLA-A2-binding epitope of E7 ($E7_{11–20}$). The stimulation of CD8+ T cells with DC.E6E7p16 yielded a higher percentage of $E7_{11–20}$ peptide-specific T cells (mean of 1.2%) than the T cells stimulated with control DC.Ψ5 (mean 0.2%) or DC.E6E7 (mean 0.5%). However, there was no induction of $E7_{11–20}$ peptide-specific T cells when there were stimulated with DC.E6E7p16 co-infected with Ad.αPD1 (DC.E6E7p16.αPD1) (Figure 2).

CD8+ T cell responsiveness is inhibited when anti-PD1 is added from the priming phase of in vitro stimulation

To determine whether addition of Ad.αPD1 at the priming phase conferred a deleterious effect on the induction of specific responses, we measured the activation and turnover of T cells during the priming (first) phase of stimulation. After 12 days, bulk CD8+ T cells stimulated with either DC.Ψ5 or DC.E6E7 or DC.E6E7p16 had 14%, 10% and 12% CD69+ CD8+ T cells, respectively. However, these percentages increased to 32% and 38% when they were stimulated with DC.E6E7.αPD1 or DC.E6E7p16.αPD1, respectively. These results suggest a heightened activation status when Ad.αPD1 is present. Moreover, when we looked at T cells stimulated in the presence of Ad-αPD1 (DC.E6E7.αPD1 or DC.E6E7p16.αPD1), the percent of dead cells (zombie dye positive) increased to 53% and 60% (Figure 3A, B) compared to 23–25% dead cells in the absence of Ad-αPD1. As expected, the addition of anti-PD1 during the priming phase increased activation of T cells, as measured by CD69 expression levels, but with a concomitant decrease in survival. Since increased activation and turnover might compromise the ability to respond to a second stimulation, we evaluated the IFNγ secretion of these stimulated T cells when added to newly adenovirus-infected DC in an ELISPOT assay. CD8+ T cells generated with DC.E6E7 or DC.E6E7p16 that were re-stimulated with DC.E6E7 or DC.E6E7p16 had a 15 fold increase in IFNγ secreting T cells ($154/10^4$ IFNγ secreting cells) compared to T cells alone ($10/10^4$ IFNγ secreting cells). However, when CD8+ T cells were generated using DC.E6E7.αPD1 or DC.E6E7p16.αPD1and were then re-stimulated with DC.E6E7.αPD1 or DC.E6E7p16.αPD1 respectively, there were fewer IFNγ secreting T cells than without anti-PD1 (Figure 3C). These results suggest that addition of Ad.αPD1 at the initial priming phase of the *in vitro* stimulation (IVS) impaired the ability of the T cells to expand or to respond to a second challenge with antigen-loaded DC.

Naïve CD8 T cells are known to express both markers (CD45RA+/ CCR7+ double positive), while effector memory CD8 T cells lack both of these markers (24). Since we used bulk $CD8^+$ T cells for our experiments (naïve plus memory CD8 T cells), we evaluated the phenotype of the CD8+ T cells during the priming (initial) stimulation phase by evaluating CD45RA and CCR7 expression. We observed that the percent of naïve (CCR7+/CD45RA+) and effector memory (CD45RA− CCR7−) populations were about equally distributed amount CD8 T cells with about 37.2 % naïve vs. 35.8% effector memory after 48 hr (Supplementary Fig. 4A, representative flow cytometry of CD8+ T cells stimulated with DC.E6E7p16). However, after 12 days post-priming, the population of naïve T cells were

skewed to an effector memory phenotype with a decrease in the percent of naïve $CD8^+$ T cells to 9.44% and an increase in the percent effector memory to 76.2% of CD8+ T cells (Supplementary. Fig. 4A). These skewing was observed for all the different adenoviral-infected DC (data not shown). We then asked whether isolation of naïve versus memory CD8+ T cells before priming had a different effect on the two distinct populations. We negatively selected naïve and memory CD8+ T cell population prior to priming with adenovirus-transduced DC. We monitored the expression of CD45RA alone (Supplementary Fig. 4B) or in combination with CCR7 (Supplementary Fig. 4C) and we observed that 48 hr post-infection the naïve CD8+ T cells still had high levels of CD45RA, while the memory CD8 T cells remained CD45RA negative. However, similarly to what we observed with bulk CD8 T cells, the naïve CD8 T cells eventually lost the expression of CD45RA and CCR7, as they became effector memory CD8 T cells (Supplementary Fig. 4B and 4C). The generation of effector memory CD8+ T cells was observed regardless of whether DC.E6E7 or DC.E6E7.p16 were used (Supplementary Fig. 4C). Lastly we evaluated the activation status (CD69 upregulation) of these naïve and memory CD8 T cells after 48 hours post-initial stimulation. As shown in Supplementary figure 4D, there was a decrease in the levels of CD69 activation marker on naïve CD8 T cells in the presence of anti-PD1, while the memory CD8 T cells had similar levels of CD69 with or without anti-PD1.

DC co-transduced with Ad.E6E7p16 and Ad.αPD1 stimulate greater anti-tumor CD8+ T cell responses mainly when Ad.αPD1 is added at the re-stimulation phase of the IVS

In light of our findings regarding the detrimental effect of adding anti-PD1 at the priming phase of stimulation, we repeated the IVS conditions described above, except that Ad.αPD1 was introduced only to DC used for secondary re-stimulation [DC.E6E7.αPD1(restim) and DC.E6E7p16.αPD1(restim)]. To test the anti-tumor capability of these T cells, we used SCC-90, a naturally HPV-infected HNSCC cell line that expresses high levels of E6 and E7 and the protein p16 (6, 25). CD8+ T cells were tested for IFNγ secretion using ELISPOT and for the ability to kill tumor cells using a ^{51}Cr release assay (Figure 4A and B). Increased IFNγ responses were observed when Ad.αPD1 was added at the secondary re-stimulation phase together with either DC.E6E7 or DC.E6E7p16 [DC.E6E7.αPD1(restim) or DC.E6E7p16.αPD1(restim)], reaching statistical significance in the latter conditions (Figure 4A). We also tested the ability of CTL to lyse HPV+ HNSCC SCC-90 cells, observing significantly increased specific lysis of SCC-90 when CD8+ T cells were stimulated with DC.E6E7p16, regardless of whether Ad.αPD1 was added at the priming phase [DC.E6E7p16.αPD1(prim)] or at the re-stimulation phase [DC.E6E7p16.aPD1 (restim)], with 10–15 fold higher specific lysis than with Ad.Ψ5 control, respectively (Figure 4B). These results suggest that addition of anti-PD1 may be more beneficial when it is added sequentially during T cell stimulation and may have translation into vaccination strategies.

Ad.E6E7p16-transduced DC have decreased CDK4 protein levels and produced higher levels of IL-12 upon CD40-ligation compared to Ad.Ψ5 or Ad.E6E7-transduced DC

Since we observed better anti-tumor responses when Ad.E6E7p16 was used in comparison to Ad.E6E7 alone, we next evaluated the effects of the presence of p16 on DC function. We observed the levels of CDK4 were decreased by about half fold in DC infected with Ad.E6E7p16 and Ad.p16 when compared to Ad.Ψ5 control and Ad.E6E7, while the levels

of Cyclin D1 remained unchanged (Figure 5A and B). Moreover, when Ad.E6E7p16 and Ad.p16-transduced DC were activated by CD40L, the levels of IL-12 secretion increased by half fold over uninfected DC or Ad.Ψ5 control (Figure 5C). To further test whether the increased IL-12 secretion was due to CDK4 inhibition, we treated Ad.E6E7-transduced DC with a CDK4 inhibitor (DC.E6E7+CDK4inh) and evaluated their IL-12 secretion upon CD40L activation. We observed a significant increase in IL-12 production by these DC compared to DC.Ψ5 or DC.E6E7 alone (Figure 5C). These results suggest a possible novel role for p16 in inhibiting cell cycle proteins in DC, and promoting their maturation, and skewing towards Th1-phenotype.

Discussion

With the rising epidemic of HPV+ HNSCC and toxicity of non-specific chemoradiation, the need for new therapeutic vaccines to treat patients is a priority. In recent decades, therapeutic vaccine approaches have being tested against HPV-related cancers, especially against cervical cancer, which is more associated with HPV (26, 27). A few studies have been conducted in HPV+ HNSCC using non-oncogenic forms of E6 and E7 in conjunction with chemoradiotherapy, which demonstrated enhance clearance of HPV+ tumors in vivo (9). These pre-clinical and clinical studies have demonstrated the ability to use viral oncoproteins to induce anti-tumor responses. However, these responses could be further enhanced by the addition of other tumor-associated antigens highly expressed in HPV cancers, and harnessing immunological target molecules within the vaccine to broaden the repertoire of HPV cellular specificities. Another way to strengthen the anti-tumor immunity is to target the co-inhibitory molecule PD1 on dysfunctional, exhausted effector T cells. Blocking the interaction between PD1 and its ligand PD-L1 can enhance both virus-specific and tumor-specific T cell responses *in vitro* and enhance anti-viral and anti-tumor activity in pre-clinical and clinical trials (28–31).

In this study, we describe the development of several adenoviral vaccine vectors containing the non-oncogenic HPV 16 E6 and E7 genes inactivated, due to mutations and/or deletions that inhibit their ability to degrade p53 and Rb, respectively. Moreover, we fused these genes with the $p16^{INK4}$ gene, which is known to be highly overexpressed in HPV+ HNSCC. We also combined these vectors with an adenoviral vector expressing the anti-PD1 antibody. To evaluate whether these vaccines are immunogenic, we tested them *in vitro* using monocyte-derived DC from healthy donors as stimulators of autologous CD8+ T cells. We successfully demonstrated high expression of the fused E6E7 protein and/or E6E7p16 protein in DC, as well as secretion and binding of adenovirus-encoded anti-PD1. Next, we corroborated that the secreted anti-PD1 was able to bind to CD8+ T cells in the IVS, as observed by the blockade of PD-1 staining on CD8+ T cells by flow cytometry (Figure 1), and this blockade was to the same extend as the soluble anti-PD1. We then proceeded to use these adenoviral vectors in DC to stimulate autologous CD8+ T cells. We were able to induce HPV-specific T cells against the E7 11–20 peptide when T cells were stimulated with DC transduced with Ad.E6E7p16, but not with the Ad.Ψ5 or Ad.E6E7. However, the addition of Ad.αPD1 abrogated the induction of these HPV E7 specific T cells when combined with E6E7p16 (Figure 2). These results could be explained, in part, by our previous findings (32), were we showed that in PD1+ T cells, phenotypic skewing is a major

pathway of PD-1 suppression. We speculate that the effects of anti-PD1 are that it enhances the phenotypic bias of the PD1+ CD8 T cells to a more Th1 phenotype or improves the cytokine profile, but does not increase proliferation. Expansion of a T cell population requires active immunization, as we described here. In our system, perhaps it was because this was a single vaccination before we added anti-PD1, the anti-PD1 did not have a proliferative effect specifically in the antigen-specific T cells. The reduced induction of antigen-specific CD8 T cells in the presence of anti-PD1 prompted us to investigate the activation status (CD69 upregulation) of CD8 T cells during the initial stimulation (12 days post-priming). As expected, we observed heightened T cell activation and turnover when Ad.αPD1 was added during the initial priming phase, however, this also led to an increase in T cell turnover and hampered their responsiveness to further rounds of stimulation (Figure 3). Concurrently, we evaluated the phenotype of CD8 T cells over time during the first 12 days of stimulation. We observed a shift on the phenotype of CD8 T cells going from naïve to effector memory over time, when they were stimulated as bulk CD8 T cells (memory plus naïve) or as separate populations (Supplementary Fig 4A, 4B and 4C). Interestingly, when we tested naïve vs. memory CD8 T cells, separated prior to stimulation, we observed a slight inhibition in the activation (CD69 upregulation) on naïve CD8 T cells in the presence of Ad.αPD1, while memory CD8 T cells were stimulated to the same extend (by CD69 expression) in the presence or absence of anti-PD1 (Supplementary Fig. 4D). These results suggest a different effect of anti-PD1 on naïve versus memory CD8 T cells and it also suggest the need for more careful studies on the impact of anti-PD1 on naïve vs. memory CD8 T responses in future research studies.

According to the results shown thus far, the addition of anti-PD1 at the beginning of the IVS (initial priming phase) is having a deleterious effect on the induction of HPV-specific T cells. Therefore, we investigated whether delaying the exposure of CD8+ T cells to anti-PD1 blockade until the boosting/restimulation phase of the IVS was a more efficacious approach to enhance HPV-specific T cell responses. Remarkably, CD8+ T cells generated with Ad.E6E7p16 had better anti-tumor activity when anti-PD1 was added secondarily, i.e. at the re-stimulation phase via Ad.αPD1-transduced DC (Figure 4). These data suggest a novel strategy to deliver vaccines sequentially, by priming with the antigen-expressing adenoviral vaccine and then boosting with a combination of vaccine plus anti-PD1, particularly in the local tumor microenvironment where PD1 levels are highest, reflecting most potent T cell exhaustion (33), that could be relieved by local PD-1 blockade. Additionally, using an adenoviral vector to deliver anti-PD1 instead of a soluble anti-PD1 antibody has the advantage of high level and long-term expression without the possible side effects of systemic Ab therapy and autoimmunity (34, 35). These studies would increase the interest in combination immunotherapy using vaccine plus anti-PD1 to expand the pool of HPV-virus-specific T cells.

One important aspect of inducing effective anti-tumor immunity using DC-based therapies is the maturation and polarization of DC towards a more immunogenic, inflammatory Th1 phenotype that efficiently stimulate CTL responses (36). As mentioned previously, in normal tissues p16 is a cyclin-dependent kinase (CDK) inhibitor that prevents cell-cycle progression by inhibiting Cyclin D-CDK4/6 complex formation (11), but it also plays an important role in polarizing macrophages to a Th1 inflammatory phenotype (37). In our

study, we used the αDC1 cocktail for maturation of DC before we transduced them with the adenoviral vectors. Since we observed better responses when p16 was in the adenoviral vector (Ad.E6E7p16), we investigated the effects of p16 on mature DC. We observed decreased levels of the CDK4 in Ad.E6E7p16 and Ad.p16-transduced DC compared to Ad.Ψ5 and Ad.E6E7 (Fig. 5A, B). Moreover, we were able to induced higher Th1-polarizing cytokine IL-12 upon CD40 ligation in Ad.E6E7p16 and Ad.p16-transduced DC compared to Ad.Ψ5 and Ad.E6E7 (Figure 5C). Additionally, IL-12 secretion was increased by one and a half fold in Ad.E6E7-infected DC treated in with a CDK4 inhibitor compared to Ad.Ψ5-control infected DC (Figure 5C). These results suggest that p16 might have an anti-proliferative, pro-differentiation effect on mature DC by inhibiting the cell-cycle kinase CDK4 and this might be skewing them toward a more immunogenic Th1 phenotype. It also suggests that the presence of p16 together with E6 and E7 could have a double purpose, not only presenting HPV-specific peptides, but also inducing better immunogenic DC for therapy.

Supplementary Material

Refer to Web version on PubMed Central for supplementary material.

Acknowledgments

The authors thank the members of Dr. Pawel Kalinski's laboratory for providing us with the CD40L-expressing J558 cell line and advice on the project.

Work funded by NIH grant R01 DE019727, P50CA097190 and the UPMC/UPCI Tumor Microenvironment Center. This project used the UPCI Flow cytometry facility that is supported in part by the award P30CA047904.

References

1. Chaturvedi AK, Engels EA, Anderson WF, Gillison ML. Incidence trends for human papillomavirus-related and -unrelated oral squamous cell carcinomas in the United States. Journal of clinical oncology : official journal of the American Society of Clinical Oncology. 2008; 26:612–619. [PubMed: 18235120]
2. Hammarstedt L, Lindquist D, Dahlstrand H, Romanitan M, Dahlgren LO, Joneberg J, Creson N, Lindholm J, Ye W, Dalianis T, Munck-Wikland E. Human papillomavirus as a risk factor for the increase in incidence of tonsillar cancer. International journal of cancer. Journal international du cancer. 2006; 119:2620–2623. [PubMed: 16991119]
3. Chaturvedi AK, Engels EA, Pfeiffer RM, Hernandez BY, Xiao W, Kim E, Jiang B, Goodman MT, Sibug-Saber M, Cozen W, Liu L, Lynch CF, Wentzensen N, Jordan RC, Altekruse S, Anderson WF, Rosenberg PS, Gillison ML. Human papillomavirus and rising oropharyngeal cancer incidence in the United States. Journal of clinical oncology : official journal of the American Society of Clinical Oncology. 2011; 29:4294–4301. [PubMed: 21969503]
4. Sturgis EM, Ang KK. The epidemic of HPV-associated oropharyngeal cancer is here: is it time to change our treatment paradigms? Journal of the National Comprehensive Cancer Network : JNCCN. 2011; 9:665–673. [PubMed: 21636538]
5. Munger K, Baldwin A, Edwards KM, Hayakawa H, Nguyen CL, Owens M, Grace M, Huh K. Mechanisms of human papillomavirus-induced oncogenesis. Journal of virology. 2004; 78:11451–11460. [PubMed: 15479788]
6. Albers A, Abe K, Hunt J, Wang J, Lopez-Albaitero A, Schaefer C, Gooding W, Whiteside TL, Ferrone S, DeLeo A, Ferris RL. Antitumor activity of human papillomavirus type 16 E7-specific T cells against virally infected squamous cell carcinoma of the head and neck. Cancer research. 2005; 65:11146–11155. [PubMed: 16322265]

7. Monie A, Tsen SW, Hung CF, Wu TC. Therapeutic HPV DNA vaccines. Expert review of vaccines. 2009; 8:1221–1235. [PubMed: 19722895]
8. Bosch FX, Broker TR, Forman D, Moscicki AB, Gillison ML, Doorbar J, Stern PL, Stanley M, Arbyn M, Poljak M, Cuzick J, Castle PE, Schiller JT, Markowitz LE, Fisher WA, Canfell K, Denny LA, Franco EL, Steben M, Kane MA, Schiffman M, Meijer CJLM, Sankaranarayanan R, Castellsague X, Kim JJ, Brotons M, Alemany L, Albero G, Diaz M, de Sanjose S, Comprehensive IM. Comprehensive Control of Human Papillomavirus Infections and Related Diseases. Vaccine. 2013; 31:1–31.
9. Wieking BG, Vermeer DW, Spanos WC, Lee KM, Vermeer P, Lee WT, Xu Y, Gabitzsch ES, Balcaitis S, Balint JP Jr, Jones FR, Lee JH. A non-oncogenic HPV 16 E6/E7 vaccine enhances treatment of HPV expressing tumors. Cancer gene therapy. 2012; 19:667–674. [PubMed: 22918471]
10. Lee DW, Anderson ME, Wu S, Lee JH. Development of an adenoviral vaccine against E6 and E7 oncoproteins to prevent growth of human papillomavirus-positive cancer. Archives of otolaryngology--head & neck surgery. 2008; 134:1316–1323. [PubMed: 19075129]
11. Sharpless NE. INK4a/ARF: a multifunctional tumor suppressor locus. Mutation research. 2005; 576:22–38. [PubMed: 15878778]
12. Lewis JS Jr, Chernock RD, Ma XJ, Flanagan JJ, Luo Y, Gao G, Wang X, El-Mofty SK. Partial p16 staining in oropharyngeal squamous cell carcinoma: extent and pattern correlate with human papillomavirus RNA status. Modern pathology : an official journal of the United States and Canadian Academy of Pathology, Inc. 2012; 25:1212–1220.
13. Lin CJ, Grandis JR, Carey TE, Gollin SM, Whiteside TL, Koch WM, Ferris RL, Lai SY. Head and neck squamous cell carcinoma cell lines: established models and rationale for selection. Head & neck. 2007; 29:163–188. [PubMed: 17312569]
14. Doorbar J. Molecular biology of human papillomavirus infection and cervical cancer. Clinical science. 2006; 110:525–541. [PubMed: 16597322]
15. Sekaric P, Cherry JJ, Androphy EJ. Binding of human papillomavirus type 16 E6 to E6AP is not required for activation of hTERT. Journal of virology. 2008; 82:71–76. [PubMed: 17942561]
16. Patel D, Huang SM, Baglia LA, McCance DJ. The E6 protein of human papillomavirus type 16 binds to and inhibits co-activation by CBP and p300. The EMBO journal. 1999; 18:5061–5072. [PubMed: 10487758]
17. Demers GW, Espling E, Harry JB, Etscheid BG, Galloway DA. Abrogation of growth arrest signals by human papillomavirus type 16 E7 is mediated by sequences required for transformation. Journal of virology. 1996; 70:6862–6869. [PubMed: 8794328]
18. Gao W, Rzewski A, Sun H, Robbins PD, Gambotto A. UpGene: Application of a web-based DNA codon optimization algorithm. Biotechnol Prog. 2004; 20:443–448. [PubMed: 15058988]
19. Bilbao R, Reay DP, Hughes T, Biermann V, Volpers C, Goldberg L, Bergelson J, Kochanek S, Clemens PR. Fetal muscle gene transfer is not enhanced by an RGD capsid modification to high-capacity adenoviral vectors. Gene therapy. 2003; 10:1821–1829. [PubMed: 12960972]
20. Naveh HP, Vujanovic L, Butterfield LH. Cellular immunity induced by a recombinant adenovirus-human dendritic cell vaccine for melanoma. Journal for immunotherapy of cancer. 2013; 1:19. [PubMed: 24829755]
21. Vujanovic L, Ranieri E, Gambotto A, Olson WC, Kirkwood JM, Storkus WJ. IL-12p70 and IL-18 gene-modified dendritic cells loaded with tumor antigen-derived peptides or recombinant protein effectively stimulate specific Type-1 CD4+ T-cell responses from normal donors and melanoma patients in vitro. Cancer gene therapy. 2006; 13:798–805. [PubMed: 16645618]
22. Kalinski P, Schuitemaker JH, Hilkens CM, Wierenga EA, Kapsenberg ML. Final maturation of dendritic cells is associated with impaired responsiveness to IFN-gamma and to bacterial IL-12 inducers: decreased ability of mature dendritic cells to produce IL-12 during the interaction with Th cells. J Immunol. 1999; 162:3231–3236. [PubMed: 10092774]
23. Kalinski P, Wieckowski E, Muthuswamy R, de Jong E. Generation of stable Th1/CTL-, Th2-, and Th17-inducing human dendritic cells. Methods in molecular biology. 2010; 595:117–133. [PubMed: 19941108]

24. Appay V, van Lier RA, Sallusto F, Roederer M. Phenotype and function of human T lymphocyte subsets: consensus and issues. Cytometry A. 2008; 73:975–983. [PubMed: 18785267]
25. Klussmann JP, Gultekin E, Weissenborn SJ, Wieland U, Dries V, Dienes HP, Eckel HE, Pfister HJ, Fuchs PG. Expression of p16 protein identifies a distinct entity of tonsillar carcinomas associated with human papillomavirus. The American journal of pathology. 2003; 162:747–753. [PubMed: 12598309]
26. Einstein MH, Kadish AS, Burk RD, Kim MY, Wadler S, Streicher H, Goldberg GL, Runowicz CD. Heat shock fusion protein-based immunotherapy for treatment of cervical intraepithelial neoplasia III. Gynecologic oncology. 2007; 106:453–460. [PubMed: 17586030]
27. Roman LD, Wilczynski S, Muderspach LI, Burnett AF, O'Meara A, Brinkman JA, Kast WM, Facio G, Felix JC, Aldana M, Weber JS. A phase II study of Hsp-7 (SGN-00101) in women with high-grade cervical intraepithelial neoplasia. Gynecologic oncology. 2007; 106:558–566. [PubMed: 17631950]
28. Dong H, Strome SE, Salomao DR, Tamura H, Hirano F, Flies DB, Roche PC, Lu J, Zhu G, Tamada K, Lennon VA, Celis E, Chen L. Tumor-associated B7-H1 promotes T-cell apoptosis: a potential mechanism of immune evasion. Nature medicine. 2002; 8:793–800.
29. Iwai Y, Ishida M, Tanaka Y, Okazaki T, Honjo T, Minato N. Involvement of PD-L1 on tumor cells in the escape from host immune system and tumor immunotherapy by PD-L1 blockade. Proceedings of the National Academy of Sciences of the United States of America. 2002; 99:12293–12297. [PubMed: 12218188]
30. Topalian SL, Hodi FS, Brahmer JR, Gettinger SN, Smith DC, McDermott DF, Powderly JD, Carvajal RD, Sosman JA, Atkins MB, Leming PD, Spigel DR, Antonia SJ, Horn L, Drake CG, Pardoll DM, Chen L, Sharfman WH, Anders RA, Taube JM, McMiller TL, Xu H, Korman AJ, Jure-Kunkel M, Agrawal S, McDonald D, Kollia GD, Gupta A, Wigginton JM, Sznol M. Safety, activity, and immune correlates of anti-PD-1 antibody in cancer. The New England journal of medicine. 2012; 366:2443–2454. [PubMed: 22658127]
31. Pen JJ, Keersmaecker BD, Heirman C, Corthals J, Liechtenstein T, Escors D, Thielemans K, Breckpot K. Interference with PD-L1/PD-1 co-stimulation during antigen presentation enhances the multifunctionality of antigen-specific T cells. Gene therapy. 2014; 21:262–271. [PubMed: 24401835]
32. Li J, Jie HB, Lei Y, Gildener-Leapman N, Trivedi S, Green T, Kane LP, Ferris RL. PD-1/SHP-2 inhibits Tc1/Th1 phenotypic responses and the activation of T cells in the tumor microenvironment. Cancer research. 2015; 75:508–518. [PubMed: 25480946]
33. Pauken KE, Wherry EJ. Overcoming T cell exhaustion in infection and cancer. Trends Immunol. 2015; 36:265–276. [PubMed: 25797516]
34. Ascierto PA, Simeone E, Sznol M, Fu YX, Melero I. Clinical experiences with anti-CD137 and anti-PD1 therapeutic antibodies. Seminars in oncology. 2010; 37:508–516. [PubMed: 21074066]
35. Schmerling RA. Toxicity of checkpoint inhibitors. Chinese clinical oncology. 2014; 3:31. [PubMed: 25841457]
36. Figdor CG, de Vries IJ, Lesterhuis WJ, Melief CJ. Dendritic cell immunotherapy: mapping the way. Nature medicine. 2004; 10:475–480.
37. Cudejko C, Wouters K, Fuentes L, Hannou SA, Paquet C, Bantubungi K, Bouchaert E, Vanhoutte J, Fleury S, Remy P, Tailleux A, Chinetti-Gbaguidi G, Dombrowicz D, Staels B, Paumelle R. p16INK4a deficiency promotes IL-4-induced polarization and inhibits proinflammatory signaling in macrophages. Blood. 2011; 118:2556–2566. [PubMed: 21636855]

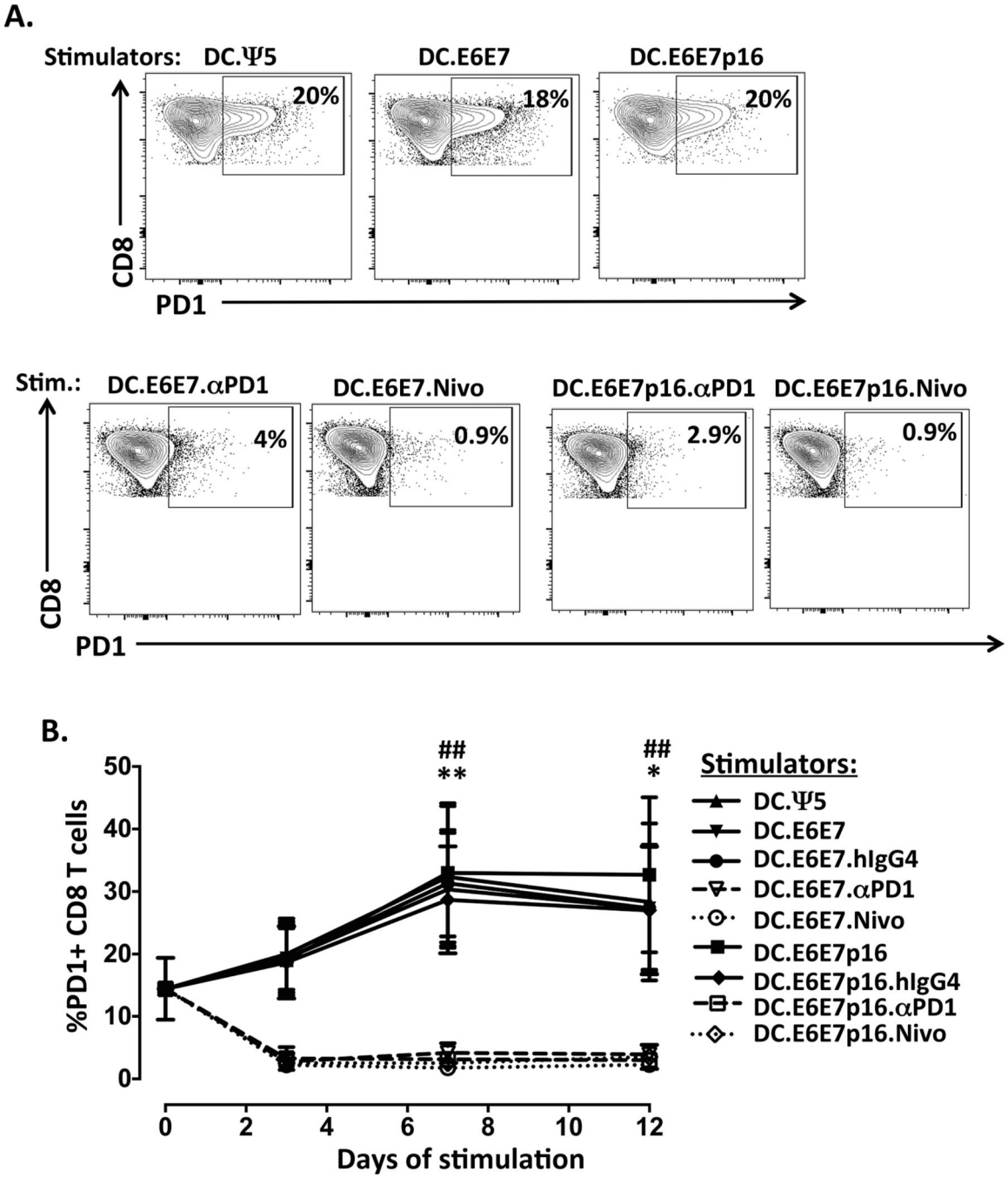

Figure 1. Adenovirus-encoded anti-PD1 effectively blocks PD1 on CD8+ T cells to the same extent as soluble anti-PD1 antibody

A) Representative flow cytometry contour plots showing the gating strategy for PD1 positive staining on day 7 *in vitro* stimulated CD8+ T cells. Boxes are defined based on fluorescence with relevant isotype control Ab. **B)** Percentage of PD1 positive CD8+ T cells during one round (12 days) of *in vitro* stimulation. DC derived from an HLA-A2+ donors were infected with either Ad.Ψ5 (DC.Ψ5), Ad.E6E7 (DC.E6E7) or Ad.E6E7p16 (DC.E6E7p16) alone or co-infected with Ad.E6E7 and Ad.αPD1 (DC.E6E7.αPD1) or

Ad.E6E7p16 and Ad.αPD1 (DC.E6E7p16.αPD1) at an MOI of 500. After 36 hrs of infection, adenovirus-transduced DCs were used to stimulate CD8+ T cells at a ratio of 1:10 (DC:T). In some cases control hIgG4 isotype (DC.E6E7.hIgG4 and DC.E6E7.hIgG4) or soluble anti-PD1 mAb (DC.E6E7.Nivo and DC.E6E7p16.Nivo) was added for comparison. CD8+ T cells were evaluated over-time for PD1 expression by flow cytometry. Results are from three separate donors. *$p<0.05$, **$p<0.01$ when DC.E6E7 was compared to DC.E6E7.αPD1 and ##$p<0.01$ when DC.E6E7.hIgG4 was compared with DC.E6E7.Nivo.

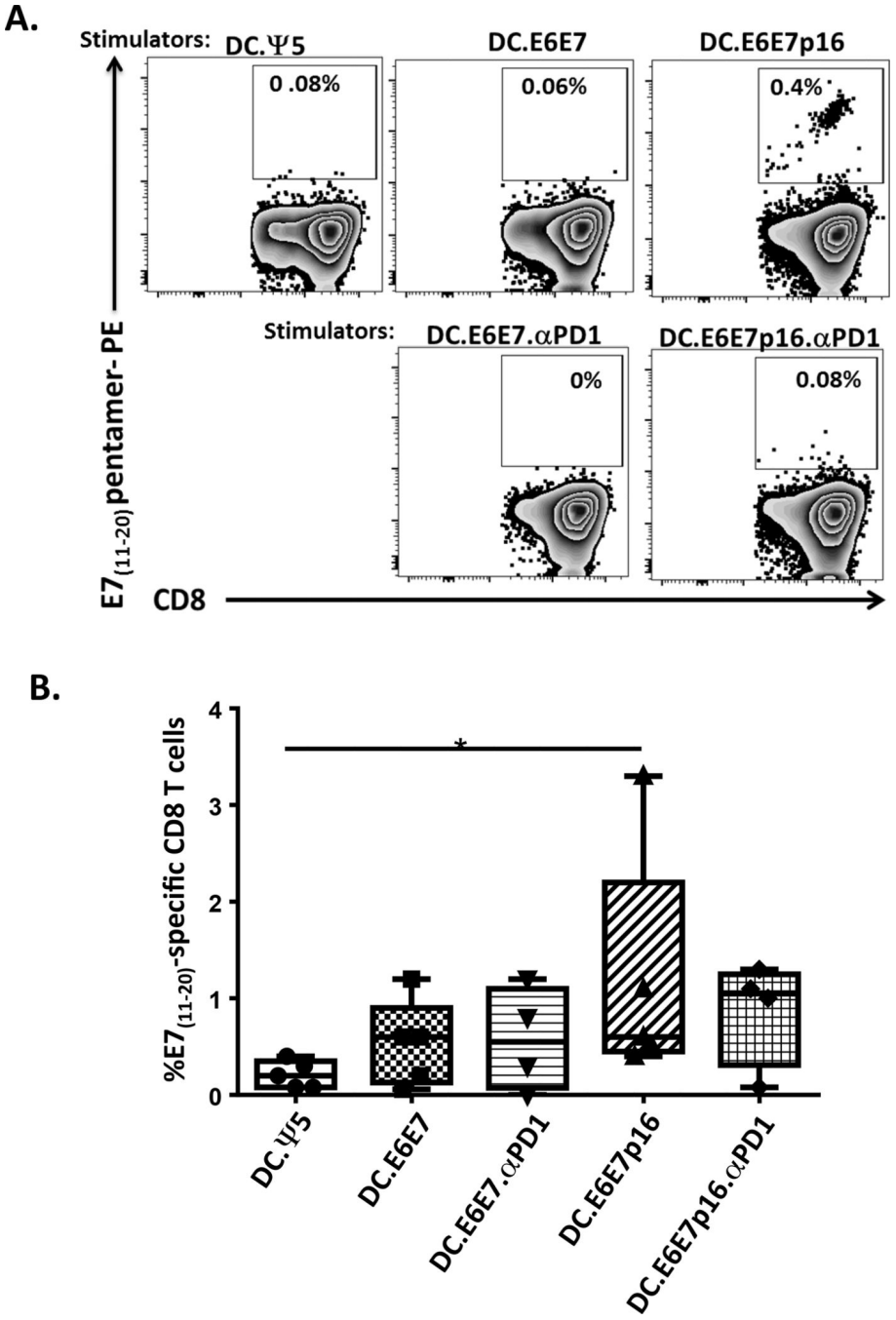

Figure 2. Evaluation of CD8+ T cell specificity after *in vitro* stimulation with autologous Ad-transduced mDCs

A) Representative plots illustrating the frequency of HLA-A2-HPV-E7$_{11–20}$ pentamer positive CD8 T cells after one round (12days) of stimulation. CD8 T cells were stimulated with DCs infected with Ad.Ψ5 (DC.Ψ5), Ad.E6E7 (DC.E6E7) or Ad.E6E7p16 (DC.E6E7p16) alone or co-infected with Ad.E6E7 and Ad.αPD1 (DC.E6E7.αPD1) or Ad.E6E7p16 and Ad.αPD1 (DC.E6E7p16.αPD1). Specific recognition was observed only when CD8 T cells were stimulated with DC.E6E7p16. B) Percentage of HPV-E7$_{11–20}$

specific CD8 T cells after 12 days of in vitro stimulation. Symbols represent individual subjects and horizontal lines represent means. *$p<0.05$

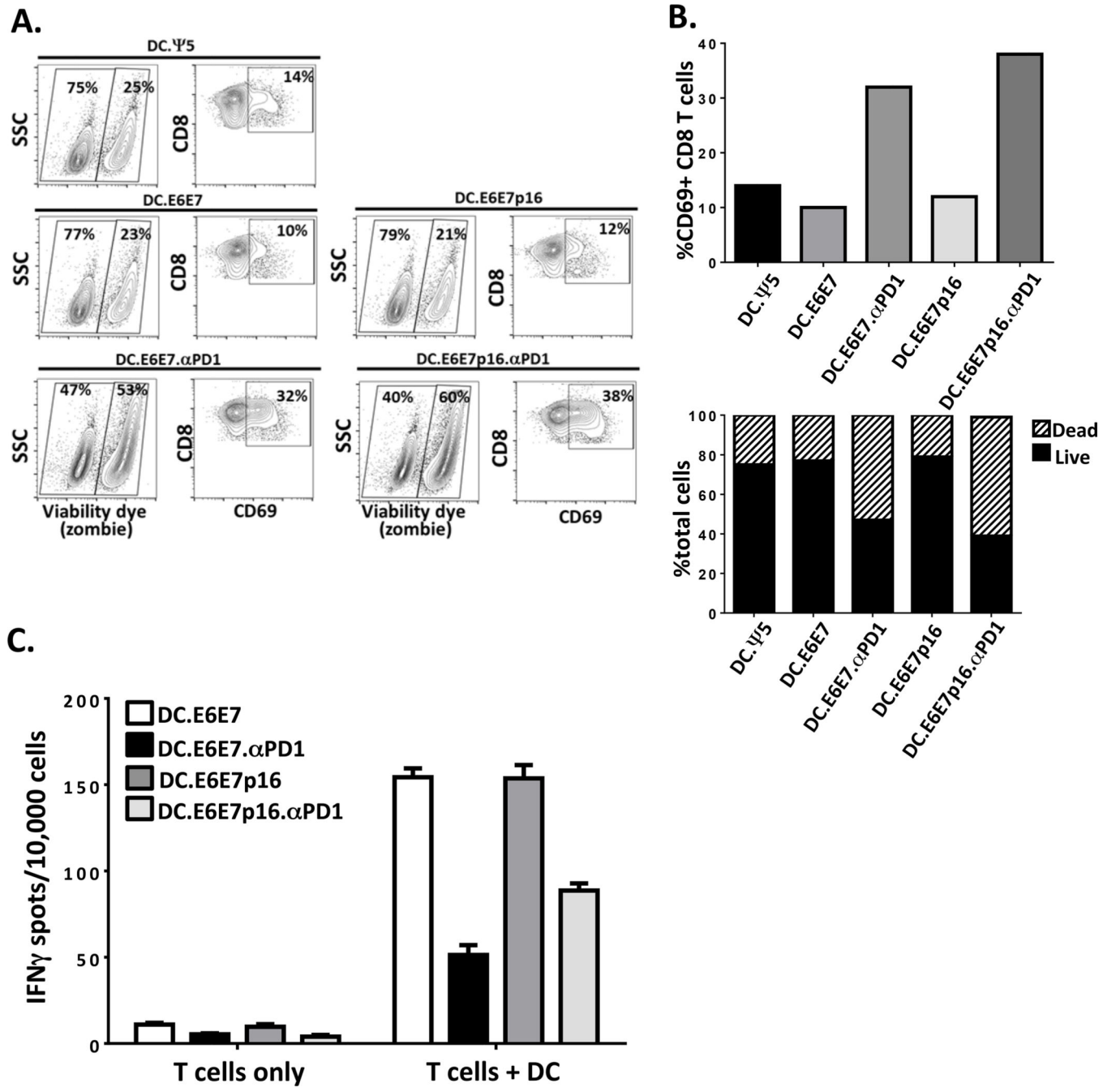

Figure 3. Increased activation and turnover of CD8+ T cells when expanded in the presence of Ad-αPD1 makes them less responsive upon re-stimulation with new adenovirus-infected DCs

A) $CD8^+$ T cells were stimulated for 12 days with either DC.Ψ5 or DC.E6E7 or DC.E6E7p16 in the presence or absence of Ad.αPD1. The percentage of dead/dying $CD8^+$ T cells was determined by using an amine reactive dye (Live/Dead) and the activation status was evaluated by the expression of activation marker CD69. **B)** Graphical representation of the percent CD69+ T cells (left graph) and the proportion of live and dead cells on each condition (right graph). **C)** Graphical representation of ELISPOT assay depicting IFNγ secreting CD8+ T cells upon re-stimulation with new adenovirus-infected DC. The number

of IFNγ secreting cells per 10,000 cells is shown. Results shown are of one representative donor.

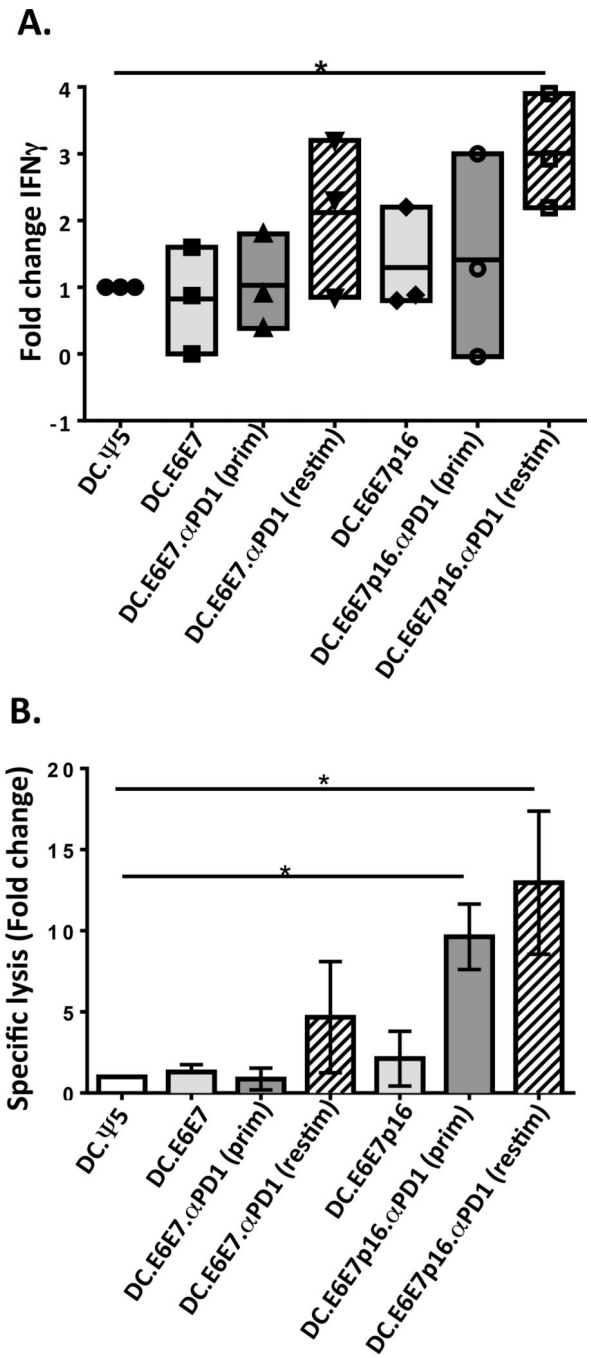

Figure 4. Dendritic cell co-transduced with Ad.E6E7p16 and Ad.αPD1 stimulate greater anti-tumor CD8+ T cell responses mainly when Ad.αPD1 is added at the re-stimulation phase of the *in vitro* stimulation

A) CD8 T cells were stimulated for 24 days (two rounds of stimulation) using autologous DC infected with Ad.Ψ5 (DC.Ψ5), Ad.E6E7 (DC.E6E7) or Ad.E6E7p16 (DC.E6E7p16) alone or co-infected with both Ad.E6E7 and Ad.αPD1 (DC.E6E7.αPD1(prim)) or both Ad.E6E7p16 and Ad.aPD1 (DC.E6E7p16.αPD1(prim)). In some cases Ad.αPD1 was only added at the re-stimulation phase on the newly adenovirus-infected DC (DC.E6E7.αPD1(restim) and DC.E6E7p16.αPD1(restim)). Responder CD8 T cells were

assessed using IFNγ-ELISPOT assays **(A)** and ^{51}Cr release killing assay **(B)** for their functional reactivity on day 24 of in vitro stimulation. IFNγ responses and specific lysis are shown as fold change over DC.Ψ5. *P<.05

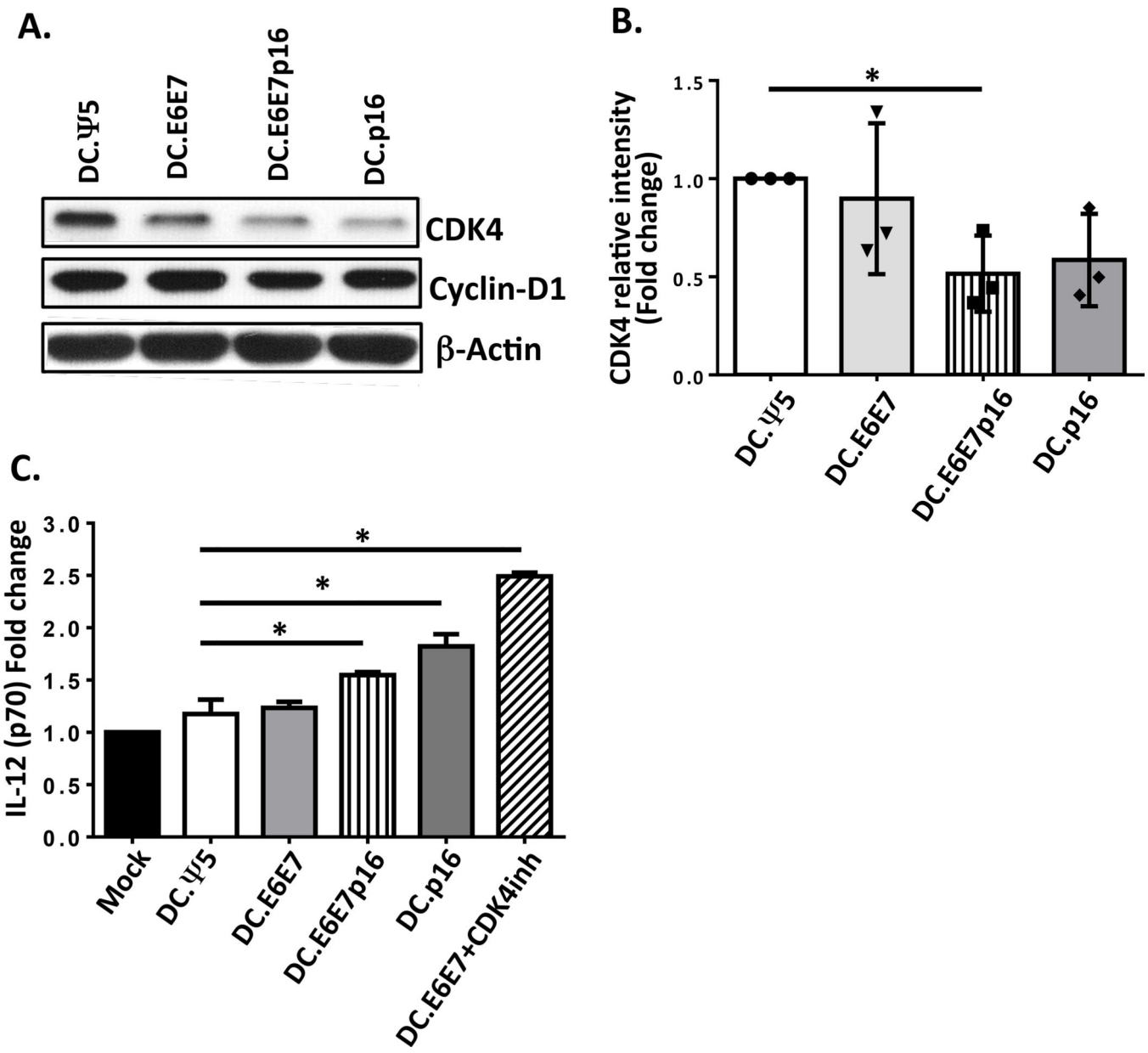

Figure 5. Ad.E6E7p16-transduced DC have decreased CDK4 protein levels and produced higher levels of IL-12 upon CD40-ligation compared to Ad.Ψ5 or Ad.E6E7-transduced DC

A) Expression levels of CDK4 and Cyclin D1 in mature DCs infected with Ad.Ψ5, Ad.E6E7, Ad.E6E7p16 and Ad.p16 were assessed 72 hr post-infection by western blot. Beta actin was used as loading control. B) Relative intensity of CDK4 expression in three different donors. Values are expressed as fold change versus Ad.Ψ5 control. C) IL-12 secretion upon CD40L stimulation of mDC left uninfected or infected with Ad.Ψ5, Ad.E6E7, Ad.E6E7p16, Ad.p16 and Ad.E6E7 plus 1 μM CDK4 inhibitor. Values are expressed as fold change over uninfected mDC. *P<.05